Available online at www.sciencedirect.com
SCIENCE DIRECT®
Journal of Photochemistry and Photobiology A: Chemistry 169 (2005) 101–107
Journal of Photochemistry and Photobiology A:Chemistry
www.elsevier.com/locate/jphotochem

Preparation and characterization of mesoporous SBA-15 supported dye-sensitized TiO_2 photocatalyst

Hanming Ding[a,b], Hong Sun[a], Yongkui Shan[a,*]

[a] *Department of Chemistry, East China Normal University, Shanghai 200062, PR China*
[b] *Shanghai Molecular Catalysis and Innovative Materials Lab, Shanghai 200433, PR China*

Received 13 December 2003; received in revised form 9 March 2004; accepted 23 April 2004
Available online 30 July 2004

Abstract

Titanium dioxide (TiO_2) is an excellent photocatalysis material for environmental purification. In order to increase the specific surface area and expand the wavelength range of excitation to visible region, dye-sensitized TiO_2 nanoparticles were fabricated onto the mesoporous silica material. In combination with sol–gel method, TiO_2, subsequently the quinacridone molecules were fabricated onto the inner pore wall of mesoporous SBA-15 silica. The hybrid material was characterized by FTIR, solid-state UV–vis spectroscopy, powder X-ray diffraction, nitrogen adsorption–desorption isotherm measurement, high-resolution TEM, and thermal analysis, respectively. The photocatalytic efficiency of such material was evaluated preliminarily. The resulting material still keeps the original hexagonal structure of SBA-15, and shows enhanced photocatalytic efficiency of decomposing indigo carmine than anatase TiO_2 and Ti-modified SBA-15 by using visible light irradiation.

Keywords: Mesoporous SBA-15; Titanium dioxide; Dye-sensitization; Photocatalysis

1. Introduction

Anatase titanium dioxide (TiO_2) is one of the excellent materials in the area of photoelectrochemical solar energy conversion and environmental photocatalysis. Photocatalytic reactions are the result of the interaction of photons having the appropriate wavelength with TiO_2 [1]. The electron-hole pair that is created upon sunlight illumination may separate and the resulting charge carriers might migrate to the surface where they react with adsorbed water and oxygen to produce radical species, thus completely decompose adsorbed organic species and metal ions. However, the efficiency of photocatalytic reactions is limited by the wide band-gap of anatase TiO_2 (3.2 eV) and the high degree of electron-hole recombination inherent in photocatalytic processes, as well as by the limited adsorption capability of photocatalysts [2]. It is well known that, in dye-sensitized TiO_2 solar cells, TiO_2 is sensitized for visible light by a monolayer of adsorbed dye to increase the overall efficiency [3]. The addition of dye molecules or other narrow band-gap semiconducting inorganic oxides in TiO_2 photocatalysts has also been proven to benefit it operation effectively on visible light illumination [1,4–13]. The principle of photosensitized degradation on TiO_2 is illustrated in Scheme 1. If the oxidation potential of the excited sensitizer is higher than the conduction band of TiO_2, following initial excitation of the adsorbed dye under visible light irradiation, electron can be injected from the excited dye into the titania particle [10,14–17]. Such charge injection process will initiate its photocatalytic reaction in a non-generation way or a regeneration by using a sacrificial electron donor [17].

For practical application, a large catalytic surface of TiO_2 photocatalyst is also necessary for the sufficient adsorption of organic polluters. It was reported that the rates of photodecomposition of gaseous NO_x [18], pyridine [19], gaseous propionaldehyde [20] and propyzamide [21] using TiO_2 photocatalysts were enhanced by loading TiO_2 particles onto

* Corresponding author. Fax: +86 21 52510411.
E-mail address: ykshan@chem.ecnu.edu.cn (Y. Shan).

1010-6030/$ – see front matter © 2004 Elsevier B.V. All rights reserved.
doi:10.1016/j.jphotochem.2004.04.015

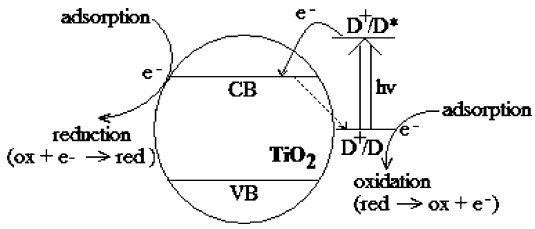

Scheme 1. Photosensitized degradation reaction on sensitized TiO_2 particle. D stands for sensitizer; D*, electronically excited sensitizer; D^+, oxidized sensitizer. The charge injection from excited sensitizer (D*) into conduction band (CB) of a large bandgap semiconductor initiates its photocatalytic reaction.

adsorbents such as zeolite, silica, and activated carbon. The possible reason is that the adsorbent support concentrates a target substrate on its surface, providing the substrate-rich environment at the adsorbent/TiO_2 interface. By using mixed SiO_2 and TiO_2 also resulted in enhanced photocatalytic efficiencies in the destruction of rhodamine-6G [8] and ethylene [22] compared with Degussa P-25 TiO_2 alone. The beneficial effect of SiO_2, which shows no photoactivity, probably relates to the preferential adsorption of the substrates on SiO_2. And Chen et al. [23] suggested that the doping of SiO_2 had no effect on the crystal structure and the surficial group of TiO_2, except for increasing specific surface area. Thus, it can be concluded that increasing the specific surface area of TiO_2 is one of the ways to improve its photocatalytic efficiency. Several kinds of methods can be pursued to increase the specific surface area of TiO_2, including production of thin films [24], preparation of TiO_2 molecular sieves [25,26], immobilization of TiO_2 into porous materials [27,28]. Recently, TiO_2 has been introduced into mesoporous silica such as MCM-41 and SBA-15. Two main types of Ti(IV)-modified mesoporous materials have been prepared: one is the Ti species were incorporated into the framework, and another is the titanium dioxides were grafted onto the internal surface [29]. In recent, Aronson et al. used $TiCl_4$ in hexane to graft titania clusters within the pores of MCM-41, which was active in the photodegradation of rhodamine-6G [30]. Morey et al. [31] and Zheng et al. [32,33] employed titanium isopropoxide in hexane under inert atmospheric conditions to graft titania inside the pores of MCM-41 or SBA-15. As titanium-containing mesoporous materials have higher active surface areas than pure titania does, these materials are expected to have enhanced photocatalytic efficiencies [30–33].

In the present paper, we used tetraethoxy titanium in methanol/toluene mixture to fabricate TiO_2 onto the inner walls of SBA-15, and subsequently deposited organic dye molecules onto the surfaces of TiO_2. Herein we chose quinacridone as the dye molecule, due to its outstanding fastness property, a high degree of thermal and chemical stability and insolubility in water. The structure and photocatalytic activities of the as-synthesized materials have been evaluated.

2. Experimental

2.1. Materials and sample preparation

Poly(ethyleneoxide)-*b*-poly(propyleneoxide)-*b*-poly(ethyleneoxide) ($EO_{20}PO_{70}EO_{20}$) was purchased from Aldrich. SBA-15 mesoporous molecular sieves were prepared by using the hydrothermal method, according to the literature [34]. Tetraethoxy titanium (IV) (TEOT), tetraethoxysilane and other chemicals used herein were purchased from Shanghai Chemical Reagent Ltd. After dehydrated in vacuum, 1.0 g calcined SBA-15 was mixed with 50 mL methanol in a flask. Then 10 mL 0.05 mol/L TEOT methanol/toluene (1:1 in volume) solution was added dropwise into the mixture under vigorous stirring. The resulting mixture was stirred at room temperature for 48 h. The solid product was separated from the mixture using centrifugation and was washed with methanol until un-reacted TEOT was removed, before being dried in vacuum. The titanium-modified sample was denoted as Ti-SBA-15. A total of 0.5 g of Ti-SBA-15 was mixed with 25 mL of acidic methanol solution, and then 10 mL of 0.01mol/L 2,9-dichloroquinacridone (abbreviated as DCQ) methanol solution was added under stirring. The mixture was further stirred for 24 h at room temperature, followed by separation with centrifugation and washing with methanol and water. The solid product was dried at room temperature in vacuum. This sample was denoted as DCQ-Ti-SBA-15.

2.2. Characterization techniques

Fourier transform infrared (FTIR) spectra were recorded from KBr pellets or with a diffuse reflectance accessory in a Nicolet Nexus 670 spectrophotometer. Solid-state diffusion-reflectance UV–vis spectra were recorded with a PE Lambda UV–vis spectrophotometer equipped with an integrating sphere diffuse reflectance accessory, using polytetrafluoroethylene as reference scatter. Powder samples were loaded into a quartz cell and spectra were collected in the range of 200–800 nm. Powder X-ray diffraction (XRD) patterns were acquired on a Bruker D/8 ADVANCE diffractometer using Cu K_α radiation (λ = 1.54178 Å) and Ni filter. The Brunauer–Emmett–Teller (BET) surface areas and pore volumes of the samples were determined from the N_2 adsorption–desorption isotherms at 77 K using a Quantachrome Autosorb 5e automated gas sorption system. All sample were evacuated for 2 h at 60 °C prior to adsorption. The specific surface area was determined by the standard BET method. For the determination of the pore size distributions, the Barrett–Joyner–Halenda (BJH) model was applied assuming a cylindrical geometry of the pores. High-resolution transmission electron microscopy (HRTEM) and energy disperse spectrum were performed using a Japan JEOL JEM2011 HRTEM operating at 120 kV. All the studied samples were dispersed in acetone by ultrasonic treatment and placed on a carbon-coated copper grid. Thermal gravimetric-differential thermal gravimetric analysis

(TGA-DTA) was carried out by using a Mettler 851e TGA/SDTA analyzer. TGA and DTA measurements were carried out under a nitrogen atmosphere from 303 to 1073 K with a heating rate of 10 °C/min.

2.3. Photocatalytic evaluation

The photocatalytic runs were carried out in a homemade reactor with a beaker containing the aqueous dispersion of the catalyst and indigo carmine. The reactor was surrounded with a cooling system to keep the temperature at 25 °C during the reaction. All the irradiation runs were performed with a 500 W cannular tungsten halogen lamp (luminous flux: 8500 lm) inside a quartz jacket, coaxial with the photoreactor within the reaction mixture. For comparison of the photocatalytic activity of the prepared samples, in all experiments the amount of indigo carmine was adjusted to achieve a concentration of 20 mg/L, and an optimum concentration of catalyst of 4 g/L was used. The decomposition of indigo carmine was monitored with its absorbance at 590 nm. Aqueous solutions of HCl and NaOH were used for adjusting the initial pH of the reaction mixture, which was kept at 3.50 in all the cases. Prior to every photocatalytic run, the reaction mixture consisting of an aqueous solution containing indigo carmine and the catalyst was magnetically agitated without illumination for at least 30 min to ensure a full adsorption of the indigo carmine molecules inside the catalyst. When the lamp was switched on, the mixture was stirred continuously and kept at 25 °C. Aliquots of 1 mL were taken at selected reaction times (every 20 min) following centrifugation before being analyzed.

3. Results and discussion

SBA-15 possesses a highly ordered large mesopores with hexagonal structure varying from 60 to 300 Å in mesopore diameter [34], which is thus an excellent candidate for supporting large complexes, even nanoparticles. In the present study, dye-sensitized TiO_2 inorganic-organic hybrid material was fabricated on the inner pore walls of SBA-15. The first step is the controlled condensation and/or grafting of TEOT via the pendant Si–OH groups on the inner walls of SBA-15. No water is present at this stage in order to prevent hydrolysis of TBOT. Then DCQ molecules were introduced onto the surface of titanium species. As their insolubility in most organic solvents, DCQ molecules were dispersed into ethanol and then were added into the Ti-SBA-15/ethanol mixture. After stirring for 3 h, the precipitation was separated, washed completely and dried in vacuum. In this case, DCQ molecules may be adsorbed into Ti-SBA-15 via chemisorption or physisorption. If the solid DCQ-Ti-SBA-15 was added into dimethylformamide (DMF), some DCQ molecules were soluble in DMF after ultrasonication for 1 h, based on the apparent color change. This fact suggests that some DCQ molecules were absorbed onto mesoporous Ti-SBA-15 physically, while other molecules were anchored via chemical bonds.

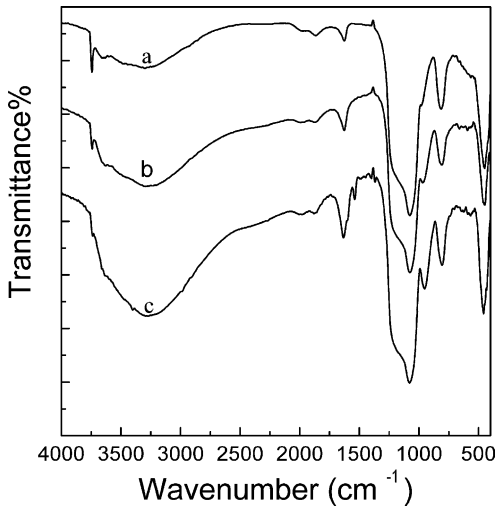

Fig. 1. FTIR spectra of SBA-15 (a), Ti-SBA-15 (b), and DCQ-Ti-SBA-15 (c).

Infrared spectroscopy was used to monitor the growth of the nanohybrid materials inside SBA-15, which can yield valuable information about the framework of SBA-15 and the local bonding environment in the modified SBA-15 samples. The spectra of all the samples are shown in Fig. 1. The broad band from 3400 to 3700 cm^{-1} is assigned to stretching frequencies of hydrogen bound silanols, while the sharp band at 3742 cm^{-1} is assigned to isolated SiO–H stretches [35]. After modified with TEOT, the intensity of the sharp band decreases markedly, as shown in Fig. 1b, suggesting the successful attachment of titanium species on the pore walls of SBA-15. In all the spectra, bands at 1080 and 801 cm^{-1} are attributed to the asymmetric and symmetric stretching vibrations of framework Si–O–Si, respectively. The Si–O–Ti antisymmetric stretching band appears at 940 cm^{-1} when $=Ti(OEt)_2$ groups were grafted on the pore walls of SBA-15 [31], which also evidenced the anchor of titanium species on the wall of SBA-15. The less of crystalline TiO_2 inside SBA-15 is confirmed, since there is a very weak stretching band at 710 cm^{-1} assignable to Ti–O–Ti, which is formed between the more numerous titanium centers [36]. This fact hints that the titanium species maybe exist as very fine oxide nanoparticles on the pore wall of SBA-15. There are new features appearing at the range of 1500–1300 cm^{-1} when the DCQ dye molecules were anchored on the surface of titanium species. New bands appearing at 1537, 1490, 1446, and 1370 cm^{-1} are assigned to the vibrations of quinacridone molecules. The bonding of dye molecules with Ti-SBA-15 is not exactly clear at present. Maybe the hydrogen bonds between quinacridone and titanyl groups are responsible for it [37]. The color change from light yellow to red after surface functionalization also provides evidence for the incorporation of dye molecules into Ti-SBA-15, even under a long-time wash with DMF under ultrasonication.

Solid state UV–vis spectroscopy further evidenced the formation of the desired materials. UV–vis spectra of the

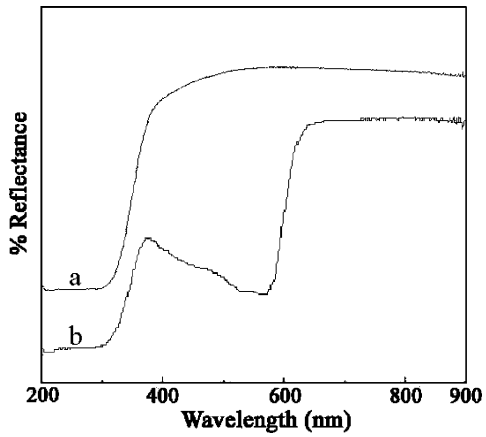

Fig. 2. UV–vis spectra of Ti-SBA-15 (a) and DCQ-Ti-SBA-15 (b).

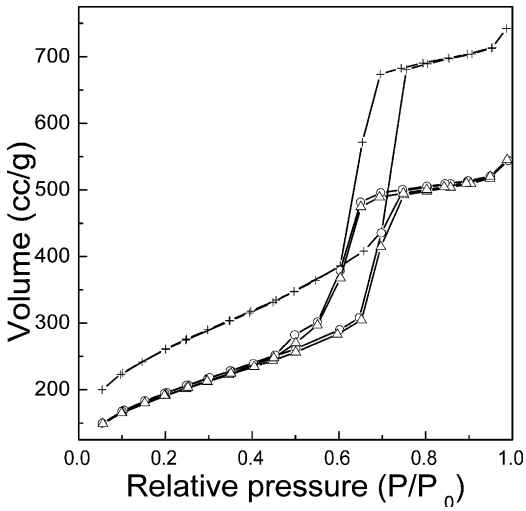

Fig. 3. Nitrogen adsorption–desorption isotherms of SBA-15 (+), Ti-SBA-15 (◯) and DCQ-Ti-SBA-15 (△).

Ti-SBA-15 before and after surface functionalization with dye molecules are shown in Fig. 2. As there is no absorptions arising from silica, which is transparent in this region exemplified by UV–vis spectrum of SBA-15, the band edge of 300 nm observed in Fig. 2a comes from titanium species. This band edge is significantly blue shifted from the one of pure anatase, showing the well-known quantum size effect for semiconductors. For TiO_2 particles, it has been reported that the absorption edge increases with dispersion from about 300 nm for nanoparticles up to 360–370 nm for bulk anatase [38]. The absorption around 300 nm indicated that TiO_2 nanoparticles are formed during grafting. After the surface functionalization with quinacridone molecules, a new band at 580 nm emerges. The red shift of the UV–vis absorbance edge in titanium-modified samples is due to the surface-modification of the dye molecules, which will benefit the samples to absorb visible light.

The XRD pattern of SBA-15 exhibits three peaks of (1 0 0), (1 1 0), and (2 0 0), which is the characteristic of a highly ordered hexagonal structure [34]. This observation is in agreement with that of previous reports on the same type of materials. Ti-SBA-15 and DCQ-Ti-SBA-15 samples show the similar XRD characteristic to the one of SBA-15. The (1 0 0) Bragg reflections could be indexed to a hexagonal unit cell, a = 114.6 Å ($2d_{100}/\sqrt{3}$) for SBA-15, a = 115.9 Å for Ti-SBA-15, and a = 118.6 Å for DCQ-Ti-SBA-15, respectively [34,39]. The near retention of the unit cell indicates that the structure is maintained upon the grafting of titanium and further incorporation of dye molecules, confirming that the hexagonal SBA-15 is stable. It is believed that the presence of titania on the pore walls introduced defects that could lead to collapse of the framework, which decreased the peak intensity of (1 0 0) in titanium-modified samples, in comparison to unmodified MCM-41 [30]. In our case, the intensity of (1 0 0) keeps unchanged, except a slightly shift of 2θ value, suggesting that the introduction of Ti species do not destroy the structure of SBA-15.

Nitrogen adsorption–desorption isotherms of the SBA-15 samples are present in Fig. 3. The isotherm of the SBA-15 matches very well the reported one and presents a type IV isotherm [34]. The type IV isotherm with H1-type hysteresis is typical of mesoporous materials with one-dimensional cylindrical channels. The sharp inflection between the relative pressures P/P_0 0.7 and 0.8 in this isotherm corresponds to capillary condensation within uniform mesopores. The sharpness of this step reflects the uniform pore size in this material. A mean pore size of 68 Å calculated on the desorption branch of the isotherm according to the standard BJH method, a pore volume of 1.148 cm^3/g, and a BET surface area of 924.4 m^2/g are obtained from the isotherm of SBA-15. These values become smaller after the grafting of titanium species on the pore walls of SBA-15, as indicated in Table 1. The reduction in size is especially reflected in the BET surface area, which showed a reduction of about 27%. The observation of the decreased surface area may be an indication of the formation of TiO_2 clusters within the mesopores. In addition, after the functionalization of DCQ molecules on the surface of pore walls of

Table 1
Physico-chemical properties of all the SBA-15 samples

Sample	d_{100} (Å)	BET surface area (m^2/g)	Pore size (Å)	Pore volume (cc/g)	Wall thickness (Å)
SBA-15	99.3	924.4	67.8	1.148	46.8
Ti-SBA-15	100.4	674.8	53.2	0.842	62.7
DCQ-Ti-SBA-15	102.7	659.5	53.9	0.844	64.7

The value of d_{100} comes from XRD measurement. Pore size distributions, pore volumes, and BET isotherms were determined from N_2 adsorption–desorption experiments. The wall thickness was calculated as: ($2d_{100}/\sqrt{3}$) − pore size [34].

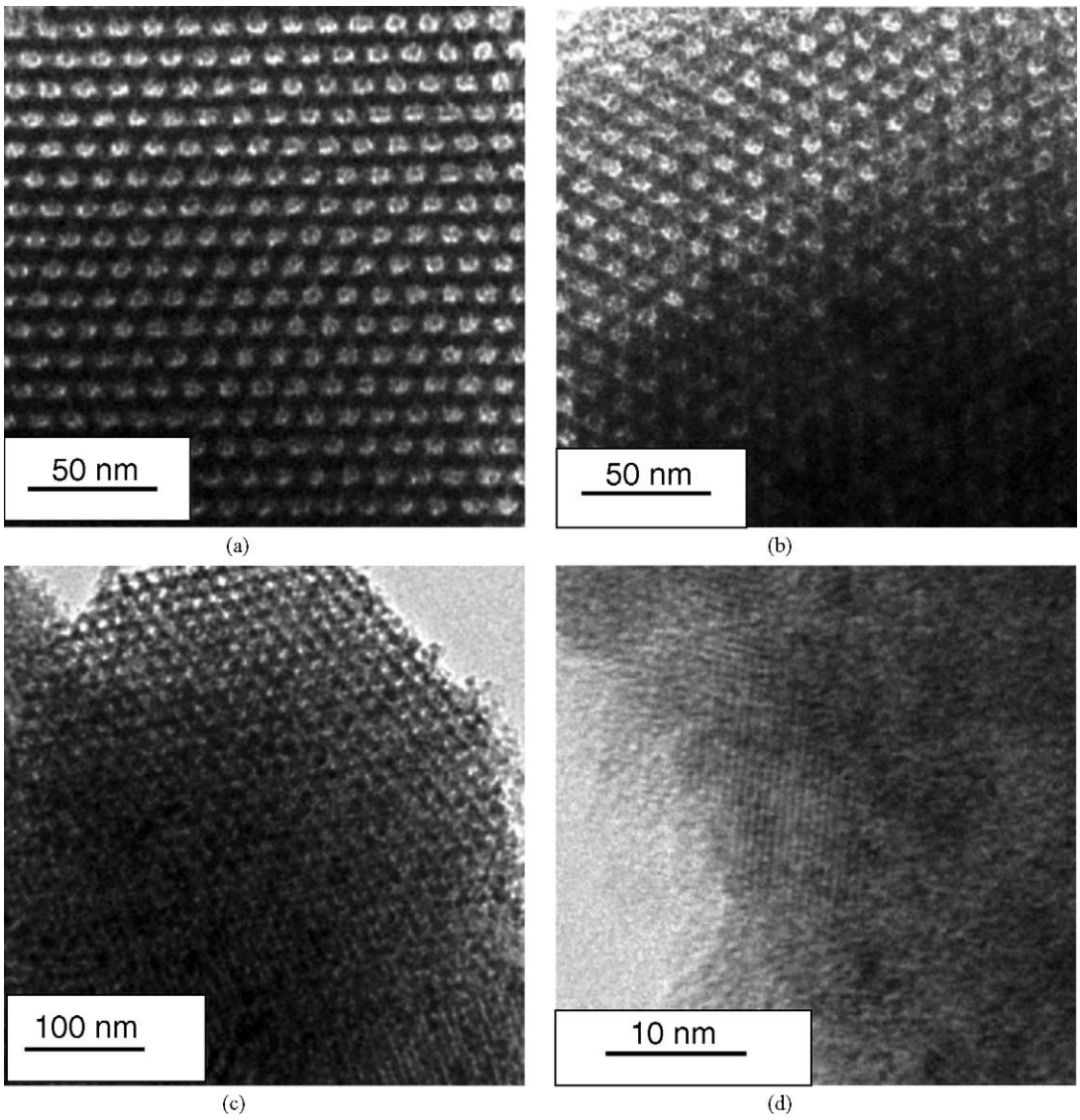

Fig. 4. HRTEM images of SBA-15 (a), Ti-SBA-15 (b), and DCQ-Ti-SBA-15 (c) recorded along the direction of the pore axis, and pore wall of Ti-SBA-15 (d).

Ti-SBA-15, there is a small change in the above values. This fact implies that a few of the dye molecules are bound to the titania surface of pore walls, while most of them are adsorbed onto the outer surfaces of Ti-SBA-15. This fact is also proved by the change in the wall thickness, as indicated in Table 1. From the increased value of wall thickness, the thickness of titania on the pore wall of SBA-15 can be estimated to ca. 8 Å, by assuming that the totality of the surface is covered with Ti species.

HRTEM images of the SBA-15 samples are shown in Fig. 4. It shows that the highly ordered pore structure of SBA-15 has been kept after the grafting of titanium species, and further the dye molecules. TEM of the calcined sample shows that the (1 0 0) direction retains a regular hexagonal array of uniform channels characteristic of mesoporous SBA-15. Each pore is surrounded by six neighbors and is of hexagonal structure, and unaffected by the presence of titania within. The d_{100} value and the diameter of the channels as obtained from electron microscopy correspond well to the d_{100} values of the powder XRD pattern. However, crystalline TiO_2 is observed in some places, as shown in Fig. 5d, suggesting that the dispersion of titanium species is not exactly homogeneous on the pore walls of SBA-15. The energy disperse spectrum shows that the Si:Ti ratio is under 5 ± 0.5 in weight, according to the quantitation method of Cliff Lorimer thin ratio section. The Ti percent is much larger than the one of Ti-SBA-15 prepared with titanium isopropoxide in dry hexane (Si:Ti = 22:1 in weight) [31], while is similar to the one within Ti-MCM-41 prepared with tetrabutyltitanate in dry hexane [32]. This fact suggests that the grafting method has much effect on the loading of Ti species inside mesoporous silica materials.

Thermal gravimetric and differential thermal analyses (TGA and DTA) pattern of the DCQ-Ti-SBA-15 were

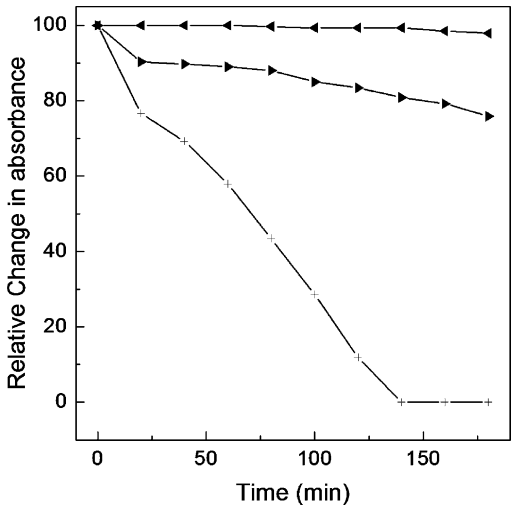

Fig. 5. Photocatalytic evaluation of DCQ-Ti-SBA-15 (+), SBA-15 (◄), and Ti-SBA-15 (►).

measured. The TGA curve revealed a total weight loss of about 40% up to 1073 K. The weight loss occurs in two main steps. The first step between 298 K and 373 K with a weight loss of 15.9% is due to the loss of molecular water and ethanol adsorbed in the mesoporous material. The second step shows a broad exothermic peak, corresponding to the decomposition of organic components. This measurement also suggests the successful loading of DCQ molecules inside the mesoporous SBA-15.

Photo-degradation reactions of indigo carmine were carried out in order to evaluate the activities of the prepared photocatalysts. Blank experiments were carried out in the absence of catalyst, and in the presence of SBA-15. No obvious photo-degradation of indigo carmine was observed in both cases (Fig. 5). Our reference experiments confirm that Ti-SBA-15 has more photocatalytic effect on the degradation of indigo carmine than anatase titania, mostly due to its porosity, higher specific surface area and more accessible photo-oxidative sites. A complete decoloration of indigo carmine could only be observed with the presence of Ti-SBA-15 or DCQ-Ti-SBA-15, thus suggesting the studied process is a photocatalytic reaction. The photocatalytic activities of Ti-SBA-15 and DCQ-Ti-SBA-15 were shown in Fig. 5 as indigo carmine degradation after 2 h. As shown in this figure, the absorption of indigo carmine solution was observably decreased just after the beginning of visible light-irradiation when DCQ-Ti-SBA-15 was used as the photocatalyst. Increasing of light-irradiation time, results in a further decrease of the absorption. The kinetics of decoloration is similar to these reported previously [40,41]. It can be clearly seen that the DCQ-Ti-SBA-15 has a better photocatalytic property than Ti-SBA-15. Herrmann [40] reported that the total decoloration of indigo carmine aqueous solution of 29.85 mg/mL (64 μmol/L) by visible-irradiated Degussa P-25 titania was reached within 16 h. These facts inferred that the dye-sensitization is responsible for the enhanced photocatalytic efficiency. Thus, as titania being quite photo-inactive under visible light, the process of the photo-bleaching has to involve the dye as a sensitizer.

Because of its large band gap, TiO_2 is only active in the ultraviolet region that is less than 10% of the overall solar light. The photosensitization process can expand the wavelength range of excitation for the photocatalyst through excitation of the dye molecules followed by charge transfer to TiO_2. Practically, some common dyes, such as porphyrin, phthalocyanine, erythrosin B, thionine, and analogs of $Ru(bpy)_3^{2+}$ have been used to degrade organic pollutants, in most cases the organic dyes serves as both a sensitizer and a substrate to be degraded [1,4–13]. Therefore, the stability of this kind of photocatalyst is not satisfied, as most of dye molecules would be photo-degraded by anatase TiO_2, thus resulting in the end of photocatalytic reaction under visible light. Recently, Chot et al. [17] used dye-sensitized TiO_2 to degrade CCl_4 under visible light in a regenerative way by using 2-propanol as a sacrificial electron donor to regenerate the sensitizer. In our present work, quinacridone dye molecules were used to sensitize TiO_2 on the inner wall surface of SBA-15. Although there is no electron donor was added, the stability of DCQ-Ti-SBA-15 on the degradation of indigo carmine was good. After five runs, the photocatalytic efficiency was nearly kept constant, suggesting this photocatalyst is quite stable. Maybe the indigo carmine photodegradation reaction provides electrons to regenerate the sensitizer molecules.

In conclusion, dye-sensitized titania materials, have been fabricated onto the inner wall of mesoporous SBA-15. A combination of FTIR, solid state UV–vis spectroscopy, XRD, HRTEM, nitrogen adsorption–desorption isotherm measurements, as well as thermogravimetry has proven that the dye-sensitized titania was deposited on both the internal and outer surface of SBA-15. The final material keeps the original hexagonal structure of SBA-15. Moreover, it shows an enhanced photocatalytic efficiency of decomposing indigo carmine than Ti-SBA-15 and anatase TiO_2 under visible light irradiation. It is reasonably considered that this result shows that it is possible to develop the high photocatalytic materials with dye-sensitized TiO_2 immobilized inside SBA-15 pores, in combination of the high specific area of SBA-15 and high photocatalytic efficiency of dye-sensitized TiO_2 on visible light illumination.

Acknowledgment

This work was supported by Natural Science Foundation of China (20273021) and Science and Technology Committee of Shanghai Municipality (0152nm049). Ding thanks financial supports from the SRF for ROCS, State Education Ministry, Shanghai Rising-Star Program (03GB14015), China.

Appendix A. Supplementary data

Supplementary data associated with this article can be found, in the online version, at doi:10.1016/j.jphotochem.2004.04.015.

References

[1] A.L. Linsebigler, G. Lu, J.T. Yates Jr., Chem. Rev. 95 (1995) 735.
[2] A. Fujishima, T.N. Rao, D.A. Tryk, J. Photochem. Photobio. C: Photochem. Rev. (2000) 1.
[3] B. O'Regan, M. Graetzel, Nature 353 (1991) 737.
[4] K. Vinodgopal, P.V. Kamat, J. Phys. Chem. 96 (1992) 5053.
[5] K. Vinodgopal, P.V. Kamat, Environ. Sci. Technol. 26 (1992) 1963–1966.
[6] A. Mills, A. Belghazi, R.H. Davies, D. Worsley, S. Morris, J. Photochem. Photobiol. A: Chem. 79 (1994) 131.
[7] H. Ross, J. Bendig, S. Hecht, Sol. Energy Mater. Sol. Cells 33 (1994) 475.
[8] C. Anderson, A.J. Bard, J. Phys. Chem. 99 (1995) 9882.
[9] K. Vinodgopal, D.E. Wynkoop, P.V. Kamat, Environ. Sci. Technol. 30 (1996) 1660.
[10] C. Nasr, K. Vinodopal, L. Fisher, S. Hotchandani, A.K. Chattopadhyay, P.V. Kamat, J. Phys. Chem. 100 (1996) 8436.
[11] J. Lobedank, E. Bellmann, J. Bendig, J. Photochem. Photobiol. A: Chem. 108 (1997) 89.
[12] F. Zhang, J. Zhao, L. Zang, T. Shen, H. Hidaka, E. Pelizzetti, N. Serpone, J. Mol. Catal. A: Chem. 120 (1997) 173.
[13] K. Kalyanasundaram, M. Graetzel, Coord. Chem. Rev. 77 (1998) 347.
[14] H. Meier, Photochem. Photobiol. 16 (1972) 219.
[15] Gerischer, Photochem. Photobiol. 16 (1972) 243.
[16] A. Hagfeldt, M. Graetzel, Chem. Rev. 95 (1995) 49.
[17] Y.M. Cho, W.Y. Choi, C.H. Lee, T. Hyeon, H.I. Lee, Environ. Sci. Technol. 35 (2001) 966.
[18] T. Ibusuki, K. Takeuchi, J. Mol. Catal. 88 (1994) 93.
[19] S. Sampath, H. Uchida, H. Yoneyama, J. Catal. 149 (1994) 189.
[20] N. Takeda, T. Torimoto, S. Sampath, S. Kuwabata, H. Yoneyama, J. Phys. Chem. 99 (1995) 9986.
[21] T. Torimoto, S. Ito, S. Kuwabata, H. Yoneyama, Environ. Sci. Technol. 30 (1996) 1275.
[22] X. Fu, L.A. Clark, Q. Yang, M.A. Anderson, Environ. Sci. Technol. 30 (1996) 647.
[23] Z. Chen, G. Yu, P. Zhang, Z. Jiang, Huan Jing Ke Xue 23 (2002) 40–44.
[24] A. Matsuda, Y. Kotani, T. Kogure, M. Tatsumisago, T. Minami, J. Sol–Gel Sci. Tech. 22 (2001) 41.
[25] R. van Grieken, J. Aguado, M.J. López-Muñoz, J. Marugán, J. Photochem. Photobio. A: Chem. 148 (2002) 315.
[26] M. Vautier, C. Guillard, J.-M. Herrmann, J. Catal. 201 (2001) 46.
[27] K. Moller, T. Bein, Chem. Mater. 10 (19982950).
[28] L. Davydov, E.P. Reddy, P. France, P.G. Smirniotis, J. Catal. 203 (2001) 157.
[29] D. Oldroyd, G. Sankar, J.M. Thomas, D. Özkaya, J. Phys. Chem. B 102 (1998) 1849.
[30] B.J. Aronson, C.F. Blanford, A. Stein, Chem. Mater. 9 (1997) 2842.
[31] M.S. Morey, S. O'Brien, S. Schwarz, G.D. Stucky, Chem. Mater. 12 (2000) 898.
[32] S. Zheng, L. Gao, Q.-H. Zhang, J.-K. Guo, J. Mater. Chem. 10 (2000) 723.
[33] S. Zheng, L. Gao, Q.-H. Zhang, W. Zhang, J.-K. Guo, J. Mater. Chem. 11 (2001) 578.
[34] D. Zhao, J. Feng, Q. Huo, N. Melosh, G.H. Fredrickson, B.F. Chmelka, G.D. Stucky, Science 279 (1998) 548.
[35] E.M. Flanigen, H. Khatami, H.A. Szymanski, Adv. Chem. Ser. 101 (1971) 201.
[36] M.A. Villegas, A. Depablos, J.M. Fernandez-Navarro, Glass Technol. 35 (1994) 276.
[37] R.M. Christie, Colour Chemistry, The Royal Society of Chemistry, Cambridge, UK, 2001.
[38] S. Klein, B.M. Veckhuysen, J.A. Martens, W.F. Maier, P.A. Jacobs, J. Catal. 163 (1996) 489.
[39] Q. Huo, D.I. Margolese, G.D. Stucky, Chem. Mater. 8 (1996) 1147.
[40] J.-M. Herrmann, Catal. Today 24 (1995) 157.
[41] M. Vautier, C. Guillard, J.-M. Herrmann, J. Catal. 201 (2001) 46.